DNA electrophoresis in a sparse ordered post array

Jia Ou, Jaeseol Cho, Daniel W. Olson, and Kevin D. Dorfman*

Department of Chemical Engineering and Materials Science, University of Minnesota–Twin Cities, 421 Washington Avenue SE, Minneapolis, Minnesota 55455, USA

(Received 23 January 2009; revised manuscript received 19 March 2009; published 4 June 2009)

We present a study of the electrophoresis of long DNA in a strong electric field through a hexagonal array of cylindrical microscale posts spaced such that the pore size is commensurate with equilibrium coil size of the DNA. Experimental mobility, dispersivity, and videomicroscopy data indicate that the DNA frequently collide with the posts, contradicting previous Brownian dynamics studies using a uniform electric field. We demonstrate via simulations that the frequent collisions, which are essential to separations in these devices, are due to the nonuniform electric field, highlighting the importance of accounting for electric-field gradients when modeling DNA transport in microfluidic devices.

DOI: 10.1103/PhysRevE.79.061904 PACS number(s): 87.15.Tt, 05.40.Fb

Microfabricated and nanofabricated devices for DNA electrophoresis promise order-of-magnitude improvements in separation time and resolution when compared to conventional pulsed-field gel electrophoresis [1]. As a general rule, the physical principles underlying DNA transport in these devices are distinctly different from the biased reptation mechanism governing DNA electrophoresis in a gel [2]. Modeling has thus played a key role in elucidating the underlying separation mechanism each time a new device has appeared [3].

As a first approximation, it is simplest to treat the electric field as a spatially uniform convective force acting on each Kuhn segment of the DNA. However, many microfluidic electrophoresis devices are constructed in oxidized silicon or glass using fabrication tools from the semiconductor industry. Alternatively, devices are replica-molded in a plastic or elastomer from a lithographically patterned substrate. In either case, the electric field in these insulating materials is nonuniform and depends strongly on the device geometry. Thus, a uniform-field model implicitly assumes that spatial variations in the electric field can be treated, in a qualitative sense, as perturbations to conclusions drawn from a uniform-field model. For example, when nonuniform electric fields have been included in models of processes such as entropic trapping [4] or the collision with an isolated post [5], the details of the chain deformation change but the qualitative mechanism remains the same—the entropic trap still traps and the DNA still collides with the post.

We show here that uniform electric-field models do not correctly capture the dynamics of long DNA in a sparse ordered microfluidic post array. Post arrays, such as the one illustrated in Fig. 1, are one of the most well-developed microfluidic methods for separating long DNA by size [6–10]. The performance of dense nanopost arrays [6–8] or slightly disordered magnetic bead arrays [9,10] is typically rationalized in the context of conclusions drawn from uniform-field models [11–14]. Our results call into question these conclusions, demonstrating the generic importance of accounting for electric-field gradients when modeling DNA electrophoresis in microfluidic devices.

*dorfman@umn.edu

The basic transport process in a sparse ordered post array is illustrated in Fig. 1(a). The separation matrix consists of a hexagonal array of cylindrical posts of diameter d and center-to-center spacing a. The DNA moves through the spacing between the posts with a velocity $v=\mu_0 E$, where μ_0 is the free-solution electrophoretic mobility and E is the average value of the electric field in the direction of net motion. The DNA molecule is characterized by its radius of gyration,

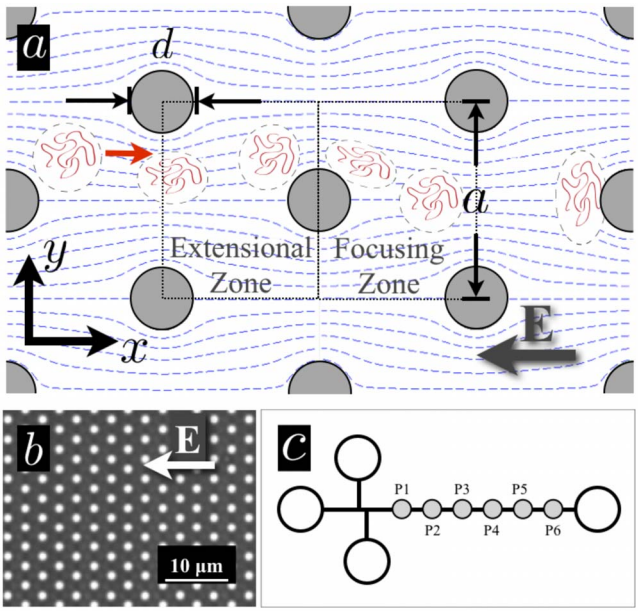

FIG. 1. (Color online) (a) Schematic illustration of a hexagonal array of cylindrical posts of diameter d and center-to-center spacing a. Several field lines created by the insulating posts are depicted in the figure. The equilibrium coil size of the DNA is commensurate with the spacing between the posts. The DNA move from left to right, in the direction opposite the electric field. (b) Image of a portion of a 50 μm$\times$15 mm PDMS hexagonal array of 1.2 μm diameter microposts with a 3 μm pitch. The electric field is applied from right to left. (c) To measure the mobility and dispersivity, the DNA are injected in a shifted-T geometry and the fluorescence intensity vs time is collected at i positions located $P_i=2.5i$ mm downstream from the injection point. The microchannel is 50 μm wide and 1.97 μm deep.

R_g, contour length, $\mathcal{L}$, and molecular diffusivity, D. By a sparse array, we mean that

$$a - d > 2R_g, \tag{1}$$

so that the spacing between the posts is large enough for the DNA to relax in the interstices.

Let us consider first the predictions of a simple uniform-field model of DNA electrophoresis in this array. As noted elsewhere [13], after a rare collision with a post, DNA in a sparse ordered array can move through the "channel" between the posts with little hindrance. Assuming that the DNA needs to align with a post by molecular diffusion, the characteristic time between collisions is the diffusive time scale, a^2/D. Thus, the DNA will proceed unhindered through the unit cell when the convection due to the electric field is strong compared to diffusion. In other words, the unit-cell Péclet number is large,

$$\mathrm{Pe} = \frac{\mu_0 E a}{D} \gg 1. \tag{2}$$

After traveling a nominal distance $l_c = \mu_0 E a^2/D$, the DNA should have also experienced a collision with characteristic hold-up time $t_c = \mathcal{L}/v$ [15]. If we define the dimensionless parameter $\gamma = \mathcal{L}/a \ll \mathrm{Pe}$, the electrophoretic mobility from this model adopts the form

$$\mu/\mu_0 = (1 + \gamma/\mathrm{Pe})^{-1} \tag{3}$$

and is approximately unity. Moreover, for an array of total length L_T, this model predicts $N_c = L_T/(a\ \mathrm{Pe})$ collisions will occur before the DNA exits the array. If N_c is not too large, then we would also expect the dispersivity of the DNA in the array, D^*, to be close to the molecular diffusivity, $D^* \approx D$. These generic conclusions, drawn from a relatively simple scaling analysis, agree with conclusions arising from Brownian dynamics simulations [13] that further account for the DNA elasticity and steric interactions between the finite-sized DNA and the post.

To test the predictions of this uniform-field model, we fabricated the polydimethylsiloxane (PDMS) post array depicted in Fig. 1(b) by soft lithography [16,17]. The electrophoresis experiments use λ-phage DNA (48.5 kbp) dyed with YOYO-1 (Molecular Probes) at 1 dye:5 bp in an electrophoresis buffer similar to Ref. [18], except that the β-mercaptoethanol was replaced with 100 mM DL-dithiothreitol. Previous experiments [19] on stained λ-DNA reported a contour length of 20–21 μm, so we will adopt $\mathcal{L} = 20.5$ μm. For the diffusivity and radius of gyration, we will use the free-solution experimental data $D = 0.47$ $\mu\mathrm{m}^2/\mathrm{s}$ and $R_g = 0.7$ μm [20]. With the latter, our post/DNA system satisfies the sparse array definition (1). Epifluorescence data were collected with a 63× oil-immersion objective using either a photomultiplier tube (Hamamatsu H7422–40) or an electron multiplying charge coupled device camera (Photometrics Cascade II).

To determine the electrophoretic mobility, μ, and dispersivity, D^*, we implemented the multi-finish-line method illustrated in Fig. 1(c) [21]. The DNA are injected in a shifted-T configuration and we measure the time, $\bar{t}$, of the maximum intensity and the full width at half maximum, τ, at different downstream distances, L. Assuming that the injected DNA plug is Gaussian at the detection point, μ and D^* can be computed from the relationships [22]

$$\frac{dL}{d\bar{t}} \sim \mu E \quad \text{and} \quad \frac{d\bar{t}_i}{d\tau^2} \sim \frac{(\mu E)^2}{(16 \ln 2) D^*}. \tag{4}$$

Importantly, the mobility and dispersivity computed by this method should be independent of the initial shape of the injection plug since they only depend on the slopes of the measured quantities. Occasionally, some experiments did not yield a linear fit (normally due to errors in the injection) and we only present data with correlation value $R^2 \geq 0.75$ when fit by Eq. (4).

For λ-DNA electrophoresis in the array in Fig. 1(b) at a nominal Péclet number of Pe=500, the uniform field model of Eq. (3) with $\gamma = 6.83$ predicts $\mu/\mu_0 \approx 0.98$ and approximately ten collisions over the 15 mm array. The latter mobility is much higher than the mobility $\mu/\mu_0 = 0.79 \pm 0.03$ we obtained by averaging our experimental data (see Fig. 3) over all fields [23].

While a reduced mobility is consistent with collisions in this ordered array, the dispersivity data presented in Fig. 2 provide much stronger support for collisions. Brownian dynamics simulations [13] using a uniform electric field predict that the dispersivity decays with Pe, asymptotically approaching the molecular diffusivity. However, the experimental dispersivity in the post array is orders of magnitude larger than what we observe in an empty channel and increases with Pe. The dispersivity in the empty channel is also slightly higher than molecular diffusion ($D^*/D \approx 10$) and increases with Pe. We attribute this behavior to the dispersion caused by transient adsorption to the PDMS surface [24],

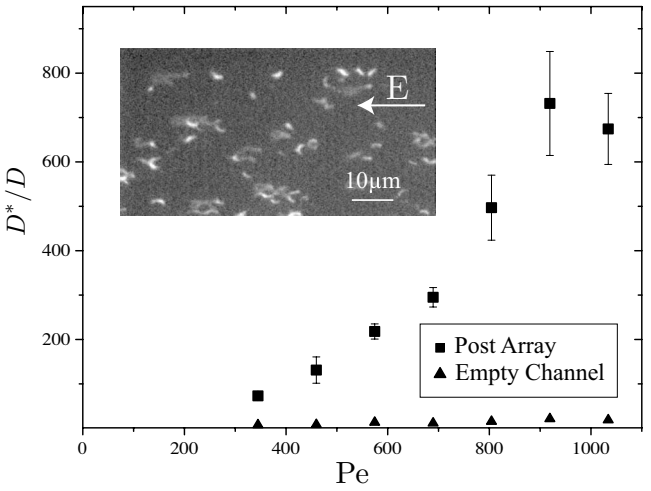

FIG. 2. Plot of the experimentally measured dispersivity, D^*, made dimensionless with the molecular diffusivity D, as a function of the Péclet number defined in Eq. (2). The squares correspond to measurements in the post array; the triangles correspond to measurements in an empty channel. The size of the error bars is one standard deviation; the error in the empty channel is smaller than the size of the symbol. The inset shows an image of the DNA dynamics at Pe=230.

which would be expected in a thin slit several R_g deep. In contrast, the large increase in the dispersion in the post array relative to the empty channel agrees with models of the dispersion due to collisions [12].

To confirm that the DNA indeed collides with the obstacles, we also imaged the DNA during electrophoresis in this array. The inset of Fig. 2 presents one frame from a movie of the electrophoresis at a somewhat lower Péclet number (Pe=230), which permits high-resolution imaging. Some of the DNA in this image are in the coiled conformation (the small bright spots); these DNA are moving between post collisions. The remaining DNA are in extended J shapes (the enlarged dim lines); these DNA are in different stages of the unhooking process. Subsequent frames in this movie show that the hooked DNA in the inset of Fig. 2 undergo the expected rope-over-pulley mechanism.

These data make clear that the DNA collide with the posts much more frequently than predicted by a uniform-field model. To rationalize this result, we propose a nonuniform field model that draws analogies between the electric field and the equivalent potential flow in fluid mechanics. Let us consider the high-Pe trajectory of the DNA molecule in Fig. 1(a) as it passes by a post without colliding. The symmetry of the hexagonal array leads to a field line that extends from the back side of this post to a stagnation point at the front side of the next post in the x direction. The electric field on the back side of the post is curved and $E_y/E_x \gg 1$ there, so the electrophoresis toward this field line is much stronger than the electrophoresis toward the next post. The resulting focusing of the DNA increases the collision probability in two ways. First, the impact parameter approaches zero [25]; the center of mass of the DNA becomes aligned with the center of mass of the post. Second, the DNA will experience an extensional "flow" as it approaches the front side of the downstream post [5]. The combination of the focusing and extensional flow regimes leads to a time between collisions much smaller than the diffusive time scale a^2/D.

To see whether the inhomogeneous field indeed plays a key role in the DNA dynamics, we implemented Brownian dynamics simulations using either a uniform field [14] or the nonuniform field imparted by the insulating posts [26] using the parameters reported in [26]. In both cases, the λ-DNA was modeled by 37 beads connected by Marko-Siggia wormlike chain springs [27] corrected for the effective persistence length [28]. Excluded volume forces were modeled with a soft potential [29] and hydrodynamic interactions were neglected. The interactions between the DNA and the walls were treated with the Heyes-Melrose algorithm [30]. In the nonuniform field simulations, we first solved Laplace's equation by the boundary element method using constant elements. At each time step in the simulation, the electric-field vector $\mathbf{E}$ at the location of each bead was obtained by a regularization method [31]. To initialize the simulations, the DNA was relaxed in free solution, placed inside the array, and allowed to relax until fluctuations in the elongation decayed to a steady value [13]. We initially placed the DNA center of mass at three different points in the unit cell: immediately behind a post, in the center of the gap between two posts, and midway between the latter two positions. The center of mass was tracked over a distance of 400 μm and ten runs were performed for each initial position at each Péclet number.

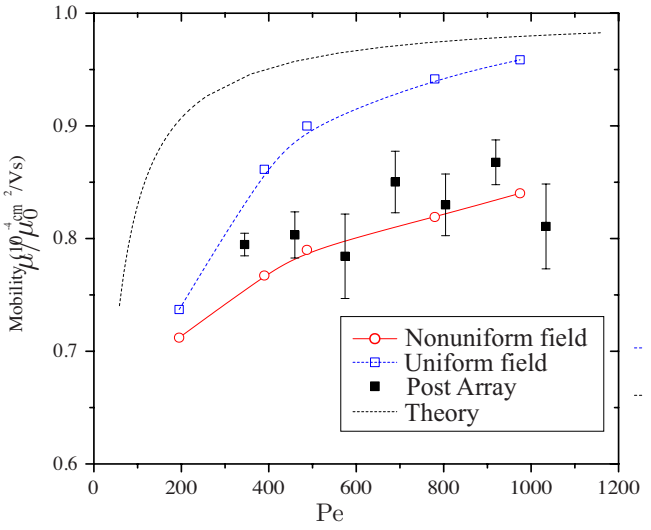

FIG. 3. (Color online) Comparison of the electrophoretic mobility, μ, made dimensionless with the free-solution mobility, μ_0, and the number of collisions as a function of the Péclet number between the experimental data (■), (ii) simulations with a nonuniform field (red, —○—), simulations with a uniform field (blue, -□-), and Eq. (3) (black, - - -). The size of the error bars for the mobility is one standard deviation; the error in the simulations is smaller than the size of the symbols. The simulation lines are only to guide the eye.

The mobilities obtained from these simulations are plotted in Fig. 3 as a function of the Péclet number, along with the experimental data. We found that the simulated mobilities were essentially independent of the initial position of the DNA, so the data in Fig. 3 represent the average over all initial conditions and all random number seeds. The uniform field model in Eq. (3) overestimates the mobility since it neglects the fact that the DNA can collide with the post with an impact parameter greater than zero [25]. The uniform field simulations are qualitatively similar to those obtained elsewhere [14] using an electric field pointing from top to bottom in Fig. 1(b). In contrast, the simulations incorporating the nonuniform field exhibit a dramatically reduced mobility. Indeed, the agreement between the latter simulations and our experimental data is quite satisfactory and confirms the importance of the nonuniform field in modeling DNA electrophoresis in sparse ordered arrays. As the inset in Fig. 3 also makes clear, the number of collisions in the nonuniform field is roughly twice that in the uniform field.

While uniform electric-field models were extremely successful at rationalizing DNA electrophoresis in gels [2], the data presented here indicate that this may not be the case for emergent microfluidic and nanofluidic devices constructed in electrically insulating materials. In the present context, prior conclusions about post arrays [11–14] need to be revisited. In a broader context, our results open the question of whether electric-field gradients have a similar impact on DNA transport in other devices with complex geometries. From a practical standpoint, the ordered arrays of micron-scale posts used here are relatively simple to fabricate by conventional

photolithography and do not require e-beam lithography [6–8] or the external equipment used to self-assemble magnetic bead arrays [9,10]. As a result, it may be possible to design more efficient separation devices by building upon the nonuniform field model presented here using tools for simulating DNA electrophoresis in complex geometries [26,32].

This work was supported by National Science Foundation Grant No. CBET-0642794 and the David and Lucile Packard Foundation. We are grateful to Michael Meloche for assistance in constructing the microscopy system. Portions of this work were performed in the University of Minnesota Nanofabrication Center, which receives partial support from the NSF through the NNIN.

[1] M. R. Mohamadi, L. Mahmoudian, N. Kaji, M. Tokeshi, H. Chuman, and Y. Baba, Nanotoday **1**, 38 (2006).
[2] J.-L. Viovy, Rev. Mod. Phys. **72**, 813 (2000).
[3] G. W. Slater, S. Guillouzi, M. G. Gauthier, J.-F. Mercier, M. Kenward, L. C. McCormick, and F. Tessier, Electrophoresis **23**, 3791 (2002).
[4] F. Tessier, J. Labrie, and G. W. Slater, Macromolecules **35**, 4791 (2002).
[5] G. C. Randall and P. S. Doyle, Phys. Rev. Lett. **93**, 058102 (2004).
[6] N. Kaji, Y. Tezuka, Y. Takamura, M. Ueda, T. Nishimoto, H. Nakanishi, Y. Horiike, and Y. Baba, Anal. Chem. **76**, 15 (2004).
[7] Y. C. Chan, Y. K. Lee, and Y. Zohar, J. Micromech. Microeng. **16**, 699 (2006).
[8] J. Shi, A. P. Fang, L. Malaquin, A. Pépin, D. Decanini, J. L. Viovy, and Y. Chen, Appl. Phys. Lett. **91**, 153114 (2007).
[9] P. S. Doyle, J. Bibette, A. Bancaud, and J. L. Viovy, Science **295**, 2237 (2002).
[10] N. Minc, C. Futterer, K. D. Dorfman, A. Bancaud, C. Gosse, C. Goubault, and J. L. Viovy, Anal. Chem. **76**, 3770 (2004).
[11] P. D. Patel and E. S. G. Shaqfeh, J. Chem. Phys. **118**, 2941 (2003).
[12] K. D. Dorfman and J.-L. Viovy, Phys. Rev. E **69**, 011901 (2004); N. Minc, J. L. Viovy, and K. D. Dorfman, Phys. Rev. Lett. **94**, 198105 (2005).
[13] A. Mohan and P. S. Doyle, Macromolecules **40**, 8794 (2007).
[14] A. Mohan and P. S. Doyle, Phys. Rev. E **76**, 040903(R) (2007).
[15] W. D. Volkmuth, T. Duke, M. C. Wu, R. H. Austin, and A. Szabo, Phys. Rev. Lett. **72**, 2117 (1994).
[16] D. C. Duffy, J. C. McDonald, O. J. A. Schueller, and G. M. Whitesides, Anal. Chem. **70**, 4974 (1998).
[17] The post array was molded from a photoresist mold (Shipley S1818) patterned by photolithography. To assemble the chips, we spin-coated a #1 coverslip with a thin film of PDMS and bonded it to the replica-molded PDMS post array after exposing both substrates to an oxygen plasma. A $1''\times 3''$ microscope slide with large cylindrical reservoirs (ID=7 mm) was bonded to the back side of the chip for reinforcement and to suppress hydrodynamic flow. The completed and sealed chips were filled with TBE 2.2× buffer and submerged in buffer for 48 h at 55 °C, a modification of an existing protocol [33] for preventing pervaporation. To perform replica experiments, the chips were regenerated by emptying them, refilling with neat buffer, and then soaking again in buffer at 55 °C.
[18] G. C. Randall and P. S. Doyle, Macromolecules **39**, 7734 (2006).
[19] G. C. Randall and P. S. Doyle, Macromolecules **38**, 2410 (2005).
[20] D. E. Smith, T. T. Perkins, and S. Chu, Macromolecules **29**, 1372 (1996).
[21] C. T. Culbertson, S. C. Jacobson, and J. M. Ramsey, Talanta **56**, 365 (2002).
[22] The electric field in the separation arm was computed from the applied potentials using Kirchoff's laws and assuming a uniform resistivity.
[23] Our measurement of $\mu_0=1.8\times 10^{-4}$ $\mathrm{cm}^2/\mathrm{V\ s}$ agrees well with previous measurements in PDMS devices [18].
[24] R. Aris, Proc. R. Soc. Lond. A Math. Phys. Sci. **252**, 538 (1959).
[25] E. M. Sevick and D. R. M. Williams, Phys. Rev. Lett. **76**, 2595 (1996).
[26] J. Cho, M. Kenward, and K. D. Dorfman, Electrophoresis **30**, 1482(2009).
[27] J. F. Marko and E. D. Siggia, Macromolecules **28**, 8759 (1995).
[28] P. T. Underhill and P. S. Doyle, J. Non-Newtonian Fluid Mech. **122**, 3 (2004).
[29] R. M. Jendrejack, J. J. de Pablo, and M. D. Graham, J. Chem. Phys. **116**, 7752 (2002).
[30] D. M. Heyes and J. R. Melrose, J. Non-Newtonian Fluid Mech. **46**, 1 (1993).
[31] H. Igarashi and T. Honma, J. Comput. Phys. **119**, 244 (1995).
[32] J. M. Kim and P. S. Doyle, J. Chem. Phys. **125**, 074906 (2006).
[33] G. C. Randall and P. S. Doyle, Proc. Natl. Acad. Sci. U.S.A. **102**, 10813 (2005).